

Determinants of Anion-Proton Coupling in Mammalian Endosomal CLC Proteins*[§]

Received for publication, October 9, 2007, and in revised form, November 16, 2007. Published, JBC Papers in Press, December 6, 2007, DOI 10.1074/jbc.M708368200

Anselm A. Zdebik^{‡§1,2}, Giovanni Zifarelli^{¶1}, Eun-Yeong Bergsdorf^{‡3}, Paolo Soliani[¶], Olaf Scheel[§], Thomas J. Jentsch^{‡§4}, and Michael Pusch^{¶5}

From the [‡]Leibniz-Institut für Molekulare Pharmakologie (FMP) and Max-Delbrück-Centrum für Molekulare Medizin (MDC), D-13125 Berlin, Germany, the [§]Zentrum für Molekulare Neurobiologie, Universität Hamburg, D-20246 Hamburg, Germany, and the [¶]Istituto di Biofisica, Consiglio Nazionale delle Ricerche, I-16149 Genova, Italy

Many proteins of the CLC gene family are Cl⁻ channels, whereas others, like the bacterial ecCLC-1 or mammalian CLC-4 and -5, mediate Cl⁻/H⁺ exchange. Mutating a “gating glutamate” (Glu-224 in CLC-4 and Glu-211 in CLC-5) converted these exchangers into anion conductances, as did the neutralization of another, intracellular “proton glutamate” in ecCLC-1. We show here that neutralizing the proton glutamate of CLC-4 (Glu-281) and CLC-5 (Glu-268), but not replacing it with aspartate, histidine, or tyrosine, rather abolished Cl⁻ and H⁺ transport. Surface expression was unchanged by these mutations. Uncoupled Cl⁻ transport could be restored in the CLC-4^{E281A} and CLC-5^{E268A} proton glutamate mutations by additionally neutralizing the gating glutamates, suggesting that wild type proteins transport anions only when protons are supplied through a cytoplasmic H⁺ donor. Each monomeric unit of the dimeric protein was found to be able to carry out Cl⁻/H⁺ exchange independently from the transport activity of the neighboring subunit. NO₃⁻ or SCN⁻ transport was partially uncoupled from H⁺ countertransport but still depended on the proton glutamate. Inserting proton glutamates into CLC channels altered their gating but failed to convert them into Cl⁻/H⁺ exchangers. Noise analysis indicated that CLC-5 switches between silent and transporting states with an apparent unitary conductance of 0.5 picosiemens. Our results are consistent with the idea that Cl⁻/H⁺ exchange of the endosomal CLC-4 and -5 proteins relies on proton delivery from an intracellular titratable residue at position 268 (numbering of CLC-5) and that the strong rectification of currents arises from the voltage-dependent proton transfer from Glu-268 to Glu-211.

CLC⁶ transport proteins are encoded by a large gene family with members in all phyla (1, 2). Because the founding member of this gene family, CLC-0, from the electric organ of *Torpedo* (3), is a chloride channel, all CLC genes were believed to encode anion channels. This is undoubtedly true for mammalian CLC-1, -2, and -K, which belong to the same homology branch as CLC-0. However, the bacterial CLC protein ecCLC-1 turned out to be an electrogenic Cl⁻/H⁺ exchanger (4). Our studies then revealed that endosomal CLC-4 and -5, which reach the plasma membrane to some degree, are Cl⁻/H⁺ exchangers as well (5, 6). The fact that several members of the gene family function as ion channels, whereas others carry out stoichiometrically coupled ion exchange, provides unprecedented opportunities to elucidate the structural basis for these different transport modes.

The linear *I/V* relationship of ecCLC-1 allowed the estimation of a 2:1 stoichiometry of transport from reversal potentials (4). Unlike ecCLC-1, CLC-4 and -5 mediate strongly outwardly rectifying currents (7), precluding a precise determination of their coupling ratio from reversal potentials. Comparing Cl⁻ and H⁺ transport rates yielded estimates for the Cl⁻/H⁺ stoichiometry between 1 and 5 (5, 6). The biological consequences of endosomal CLCs being Cl⁻/H⁺ antiporters rather than Cl⁻ channels are intriguing (8). These proteins are thought to facilitate endosomal/lysosomal acidification by neutralizing proton pump currents, a process important for endocytotic trafficking and lysosomal function. Indeed, CLC-5 is crucial for renal endocytosis and is mutated in a human disorder associated with proteinuria and kidney stones (9).

It remains unclear whether Cl⁻/H⁺ exchange depends on the dimeric structure of CLC proteins. It is known that both pores of the double-barreled CLC-0 Cl⁻ channel can be shut closed simultaneously by a “common gate” that depends on both subunits (10–13). Similarly, it may be that Cl⁻/H⁺ flux coupling in CLC transporters is based on a conformational change that involves both subunits.

Although the flux coupling is poorly understood, some amino acids involved in this process have been identified. The crystal structure of ecCLC-1 revealed a glutamate that blocks

* This work was supported in part by grants from the Deutsche Forschungsgemeinschaft (to A. A. Z. and T. J. J.) and by Telethon Foundation Grant GGP04018 (to M. P.). The costs of publication of this article were defrayed in part by the payment of page charges. This article must therefore be hereby marked “advertisement” in accordance with 18 U.S.C. Section 1734 solely to indicate this fact.

[§] The on-line version of this article (available at <http://www.jbc.org>) contains supplemental Figs. S1–S5 and Table 1.

¹ Both authors contributed equally to this work.

² Present address: London Epithelial Group, Royal Free Hospital, UCL, London NW 3 2PF, United Kingdom.

³ Fellow of the Leibniz Graduate School of Biophysics.

⁴ To whom correspondence may be addressed: MDC/FMP, Robert-Rössle-Str. 10, D-13125 Berlin, Germany. E-mail: jentsch@fmp-berlin.de.

⁵ To whom correspondence may be addressed: Istituto di Biofisica, CNR, Via de Marini 6, I-16149 Genova, Italy. E-mail: puschi@ge.ibf.cnr.it.

⁶ The abbreviations used are: CLC, a gene family of Cl⁻ channels and transporters first identified by the cloning of CLC-0 from *Torpedo*; BCECF, 2',7'-bis(carboxyethyl)-5(6)-carboxyfluorescein; MES, 2-(*N*-morpholino)ethanesulfonic acid; ecCLC-1, one of the two CLC isoforms in *E. coli*, also known as CLC-ec1; pH_i, intracellular pH; pH_o, extracellular pH; WT, wild type; HA, hemagglutinin.

Anion-Proton Coupling in Endosomal CLC Proteins

the access of external anions to a central Cl^- binding site (14). Neutralizing this glutamate created a new, more external Cl^- binding site (15). Equivalent mutations in vertebrate CLC Cl^- channels drastically changed their gating (15–17). A loss of rectification was observed with similar mutations in CIC-4 and -5 (7), which are now known to be exchangers. It was suggested (15) that this glutamate is involved in the gating by the permeant anion, a simple model explaining the voltage- and anion-dependent gating of CIC-0 (18). When this “gating glutamate” was neutralized in ecCIC-1 (4) or in CIC-4 and -5 (5, 6), proton coupling was lost, and pure anion conductances were observed. Thus, this gating glutamate has a dual role in gating CLC Cl^- channels and in coupling Cl^- to H^+ countertransport in CLC exchangers. Both roles may involve protonation and deprotonation of its side chain.

Mutations in a glutamate (“proton glutamate,” Glu-203) close to the cytoplasmic face of ecCIC-1 also uncoupled Cl^- from H^+ fluxes (19), suggesting that H^+ and Cl^- take different routes to the gating glutamate where both pathways converge. The present work on CIC-4 and -5, although showing a role of the proton glutamate in H^+ coupling, reveals important differences from ecCIC-1. Whereas neutralizing the proton glutamate converted ecCIC-1 into a Cl^- conductance, it abolished both Cl^- and H^+ transport in CIC-4 and -5. Transport of Cl^- , but not of H^+ , was restored by additionally neutralizing the gating glutamate, suggesting a strict coupling of Cl^- to H^+ transport at the central translocation site. Moreover, Cl^-/H^+ exchange is carried out independently by each subunit, and noise analysis, usually used to characterize gating events in ensembles of channels, suggests that Cl^-/H^+ exchange occurs in bursts with an apparent unitary conductance of ~ 0.5 picosiemens.

EXPERIMENTAL PROCEDURES

Molecular Biology—We employed the rat CIC-5 cDNA (20), human CIC-4 cDNA (7), *Torpedo marmorata* CIC-0 (3), and human CIC-1 (21). Concatemers were constructed employing human CIC-5 (9). All constructs were in the pTLN vector (12). Mutants were constructed by recombinant PCR and verified by sequencing. An extracellular HA tag was inserted at the equivalent position, as described by Schwake *et al.* (22), into rat WT CIC-5 and mutant constructs to quantify surface expression as described (22, 23). Briefly, live oocytes were labeled with 12Ca5 or 3F10 monoclonal antibodies (Roche Applied Science), washed, incubated with appropriate horseradish peroxidase-coupled secondary antibodies (Dianova), and extensively washed (all steps at 4 °C), and luminescence was quantified in a Turner Design TD-20/20 luminometer after placing them in ELISA Femto reagent-containing tubes (Pierce). Oocyte membranes of HA-tagged mutant CIC-5-expressing oocytes were prepared by separating the yolk from the membrane-containing supernatant through a series of centrifugation steps. Western blots were prepared according to standard procedures, and HA-tagged proteins were detected with 3F10 monoclonal antibodies. For the construction of concatemers, the 12-base pair linker ggtaccactagt was placed after the last amino acid or before the start methionine in separate

constructs. The linker codes for the amino acids GTTS. The SpeI site encoded by the last 6 bases of the linker was used for the construction of the concatemers.

Two-electrode Voltage Clamp of Injected *Xenopus* Oocytes—Oocytes were obtained by dissection and collagenase treatment of ovaries from pigmented and albino *Xenopus laevis* frogs and injected with 10–50 ng of cRNA transcribed from linearized cDNA with the Ambion mMessage mMachin kit according to the manufacturer’s instructions. Currents were measured using a standard two-electrode voltage clamp at room temperature (20–24 °C) employing a Turbo Tec amplifier (npi, Tamm, Germany) and a custom acquisition program (GePulse) or pClamp9 (Molecular Devices). The standard bath solution contained (in mM): 100 NaCl, 4 MgCl_2 , 10 HEPES, pH 7.3. Alternatively, a solution similar to frog Ringer’s was used (ND96, pH 7.5, or buffered with MES to pH 5.5 or 6.5 or with Tris to pH 8.5 as indicated), in which divalent cation and potassium salts were substituted with the corresponding gluconate salts and NaCl with NaSCN, NaNO_3 , NaBr, NaI, or NaClO_4 as indicated. Ag/AgCl electrodes and 3 M KCl agar bridges were used as reference and bath electrodes. For ion substitution experiments we substituted 100 mM NaCl with 100 mM NaSCN or 100 mM NaNO_3 and MgCl_2 with MgSO_4 .

Extracellular pH Measurements— H^+ transport activity was assessed by monitoring the acidification of the extracellular solution close to the oocyte using a pH-sensitive microelectrode as described previously (5). Briefly, a silanized microelectrode was tip-filled with a proton ionophore (Cocktail B, Fluka), backfilled with a solution containing phosphate-buffered saline, and connected to a custom high-impedance amplifier. The electrodes were routinely checked and responded consistently with a slope of 57–61 mV/pH unit. A pH-sensitive microelectrode was gently pushed onto the vitelline membrane without rupturing the plasma membrane. A microelectrode filled with 3 M KCl was placed close to the oocyte as a reference, and the difference signal was low pass-filtered at 50 Hz before digitization. The oocyte was simultaneously voltage-clamped with two microelectrodes, and acidification was induced by applying a train of voltage clamp pulses to +80 mV, as described previously (5). A pulse protocol rather than continuous depolarization was chosen to avoid the activation of endogenous conductances. CIC-4 and -5 only transport ions during the positive pulse, as they are strongly outwardly rectifying. The pH signal was averaged for the duration of one pulse of the train and plotted *versus* the time of the application of the pulse (see Fig. 1). For measurements of the extracellular acidification, solutions contained 0.5 mM buffer (HEPES for pH > 6.5, otherwise MES).

Intracellular pH Measurements—We developed a fluorescence-based device, called Fluorocyte, to measure intracellular pH changes based on the pH-sensitive excitation of BCECF (free acid, 23 nl of saturated aqueous solution injected 10–30 min prior to the experiment) at 488 nm, where fluorescence is pH-dependent. Emission was band pass-filtered at 512–565 nm, converted to current by a photodiode, and digitized by a Digidata 1320 interface (Molecular Devices) following *I/V* conversion at 0.5 V/nA. Fluorocyte allowed simultaneous two-electrode voltage clamp measurements (using an npi TEC10) and

fluorescence while perfusing the bath continuously. The oocyte was placed over a hole of 0.8 mm in diameter, through which BCECF fluorescence was measured and which was in contact with a perfusion channel. Thus, solution could be quickly exchanged both at the small membrane portion facing the hole and on the much larger rest of the oocyte. This is important for comparing currents (which reflect the conductance of the entire membrane) with changes in pH_i , which was only measured close to the plasma membrane area that faced the hole. The fluorescence response to an ensemble of depolarizing pulses to +90 mV for 400 ms interrupted by 100 ms pulses to -60 mV (to avoid the activation of endogenous currents by prolonged depolarization) was measured and digitally Bessel-filtered at 1 Hz, as in Fig. 5. The method allows a sensitive qualitative measurement of pH changes brought about by voltage clamping or solution exchange, but is not quantitative, as no ratiometric measurements and calibrations are used. We frequently observed a drift in base-line fluorescence, which became more apparent in the higher resolution scaling necessary to resolve the smaller fluorescence changes observed with weakly transporting mutants. This drift could be due to redistribution of the dye within the oocyte or bleaching, or a combination of both. However, as we observed the difference between the rate of the fluorescence change during the pulse protocol and with the oocytes held at their resting membrane potential, Fluorocyte gave a robust semiquantitative measure for H^+ transport activity.

For the anion exchange experiments aimed at a more quantitative comparison of coupling stoichiometry, we performed ratiometric BCECF imaging (excitation at 440 and 480 nm and emission between 515 and 560 nm) using a Zeiss microscope 10–30 min after injection of BCECF into the oocyte. We divided the change in ratio in response to a set of depolarizing pulses through the measured current integrated over time and normalized the data to chloride.

Inside-out Patch Clamp Measurements for Noise Analysis—The extracellular (pipette) solution contained (in mM): 100 *N*-methyl-D-glucamine Cl, 5 MgCl_2 , 10 HEPES, pH 7.3. The internal solution contained (in mM): 100 *N*-methyl-D-glucamine Cl, 2 MgCl_2 , 10 HEPES, 2 EGTA, pH 7.3. To detect macroscopic currents in excised patches, pipettes were made from aluminum silicate glass capillaries (Hilgenberg, Malsfeld, Germany) to a diameter of about 15–20 μm with a resistance of 300–800 kilohms under our recording conditions. Recordings were performed using an EPC-7 amplifier (HEKA Electronics, Lambrecht, Germany). The voltage protocol consisted of a voltage step to 140 mV for 50 ms, followed by a step to -50 mV. Currents were filtered at 20 kHz and digitized with a sampling rate of 50 kHz. Noise analysis was performed on an ensemble of 70–120 recordings. To estimate apparent “single channel” (unitary) conductances, the variance was plotted *versus* the mean current, and the points were fitted with the function (Equation 1),

$$\sigma^2 = iI - I^2/N \quad (\text{Eq. 1})$$

where i is the unitary current, I is the mean current, and N is the number of channels. Background variance was calculated at

Anion-Proton Coupling in Endosomal CLC Proteins

-50 mV and was subtracted. Power spectra were calculated from 4096 data points and averaged. They were fitted by the sum of three lorentzian components of the form (Equation 2),

$$S(f) = \frac{S_0}{1 + (f/f_c)^2} \quad (\text{Eq. 2})$$

with a cut-off frequency f_c and a low-frequency limit S_0 .

Data Analysis—Data were analyzed using custom software (Ana), SigmaPlot (SPSS Inc.), Origin (OriginLab Corporation), and pClamp9.

RESULTS

Mammalian CLC protein sequences were aligned with ecCLC-1 (Fig. 1A), and residues equivalent to ecCLC-1 Glu-148 (the gating glutamate (15)) and Glu-203 (proton glutamate (19)) are highlighted. In all members of the first homology branch (CLC-1, -2, -Ka, and -Kb), valine replaces the proton glutamate, whereas all members of the two remaining branches (CLC-3, -4, and -5 and CLC-6 and -7, respectively) retain a glutamate. Whereas the first CLC branch encodes plasma membrane Cl^- channels, CLC-3 through -7 reside mainly in the endosomal/lysosomal system (8). Of these, only CLC-4 and -5 gave plasma membrane currents large enough to ascertain their function as Cl^-/H^+ exchangers (5, 6). AtCLC-a, a NO_3^-/H^+ antiporter that accumulates nitrate in plant vacuoles (24) also displays a proton glutamate.

We therefore used CLC-4 and -5 to explore the role of putative proton glutamates in mammalian Cl^-/H^+ exchangers. As described previously (5, 6, 20), CLC-5 mediates strongly outwardly rectifying currents (Fig. 1B) and extrudes protons upon depolarization, as detected by intracellular alkalinization in Fig. 1C. Replacing the proton glutamate with the similarly acidic aspartate reduced transport activity without abolishing it (Fig. 1, D–F). The voltage dependence and kinetics of currents from the E268D mutant (Fig. 1D) resembled those of WT CLC-5 (Fig. 1B). Likewise, the mutant extruded acid equivalents when activated by trains of depolarizing pulses, as detected by intracellular alkalinization (Fig. 1E) or extracellular acidification (Fig. 1F). Importantly, and again like WT CLC-5, it could extrude protons against an electrochemical gradient (pH_o 5) (Fig. 1E), strongly suggesting a directly coupled Cl^-/H^+ exchange. The weakly basic histidine (Fig. 2A), but not the strongly basic arginine (Fig. 2B), could also functionally substitute for the proton glutamate. Tyrosine also supported Cl^-/H^+ exchange, albeit with generally lower transport rates (Fig. 2C). By contrast, when the proton glutamate was replaced with alanine, the mutants produced neither measurable currents nor H^+ transport in *Xenopus* oocytes (Fig. 1, G and H, for CLC-5_{E268A}; supplemental Fig. S1 for CLC-4_{E281A}). Likewise, no transport was observed when the proton glutamate was replaced with valine, the residue present in CLC channels, or with cysteine, methionine, or asparagine (data not shown).

To exclude that the lower transport rates exhibited by these mutants are due to a reduced abundance in the plasma membrane, we inserted an extracellular HA tag into some of these constructs and measured the protein expression on the membrane surface as described under “Experimental Proce-

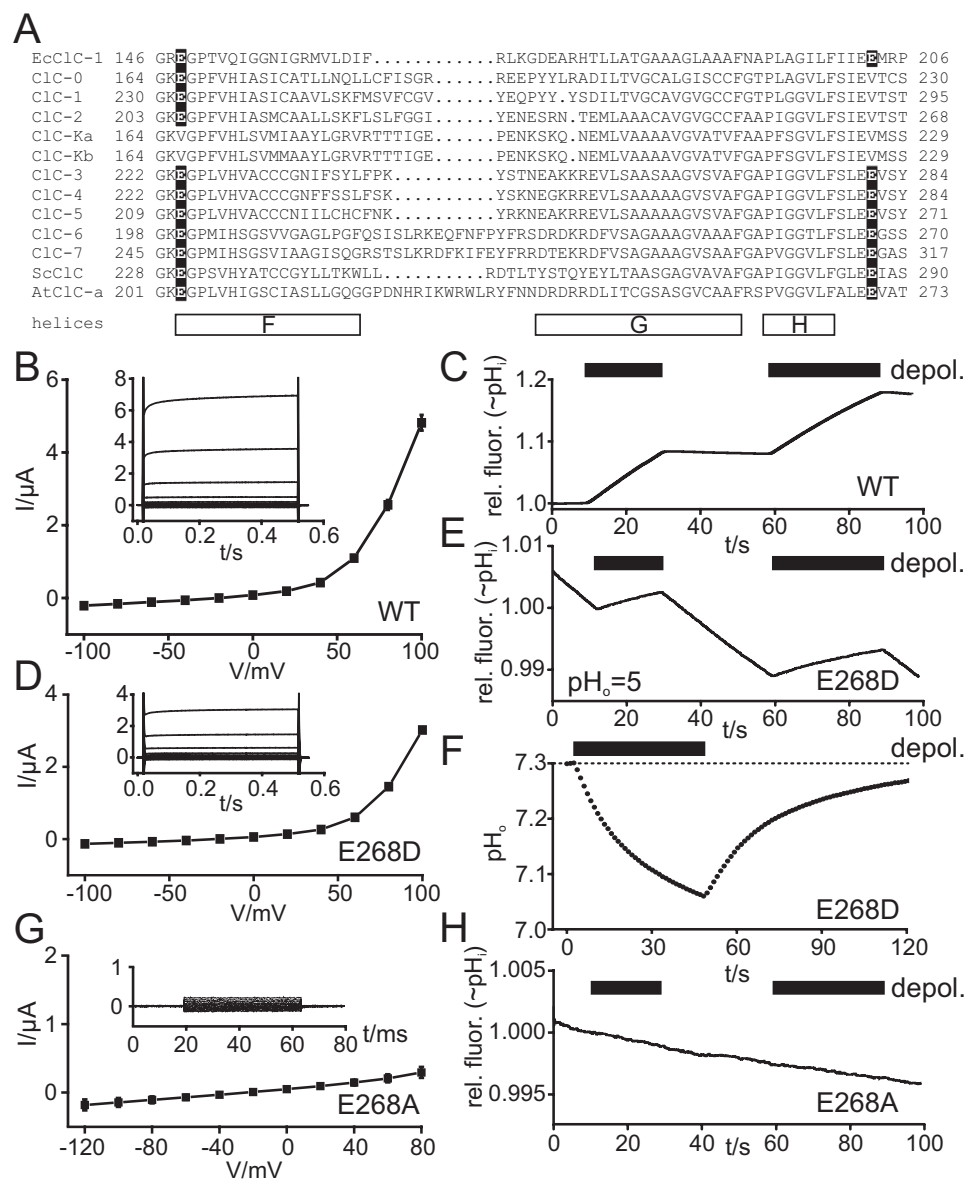


FIGURE 1. A glutamate after helix H is critical for CIC-5 Cl⁻/H⁺ exchange activity. *A*, conservation of gating (left) and proton (right) glutamates in *Escherichia coli* (*Ec*), mammalian, *Saccharomyces cerevisiae* (*Sc*), and *Arabidopsis thaliana* (*At*) CLC homologues is highlighted. Bars, intramembrane helices as revealed by the crystal structure of ecCIC-1 (14). *B* and *C*, oocyte-expressed WT CIC-5 mediates strongly outwardly rectifying currents (*B*, inset, voltage clamp traces) and H⁺ transport (*C*) as indicated by intracellular alkalization during activating trains of depolarizing pulses (*depol.*) to +90 mV (indicated by bars). BCECF fluorescence (measured by Fluorocyt) qualitatively reflects pH_i. It drifts because of bleaching or dye redistribution. *D*, CIC-5_{E268D} currents resemble WT currents, but are generally smaller. Cl⁻/H⁺ exchange is indicated by external acidification during a depolarizing pulse train to 80 mV (*n* = 5) (*F*) and by intracellular alkalization even against an electrochemical gradient of ~30 mV (90-mV pulses; pH_o 5, pH_i ~7) (*n* = 6) (*E*). *G* and *H*, mutating the CIC-5 proton glutamate to alanine (CIC-5_{E268A}) abolishes both currents (*G*, inset, voltage clamp traces) and H⁺ transport (*H*). Similar results were obtained in 17 experiments from four batches of oocytes. *rel. fluor.*, relative fluorescence.

dures." Fig. 3 shows that these mutants were present in the plasma membrane to a comparable degree. Thus the lack of transport activity of CIC-5 mutants E268A and E268R cannot be ascribed to a reduced surface expression. Western blots of total oocytes indicated similar overall expression as well (supplemental Fig. S2).

Cl⁻ currents, but not H⁺ transport, could be recovered in the proton glutamate CIC-5_{E268A} and CIC-4_{E281A} mutants by inserting an additional uncoupling mutation in the gating glutamate (Fig. 4 for CIC-5_{E211A,E268A}; supplemental Fig. S3 for

CIC-4_{E224A,E281A}). The nearly linear I/V relationship closely matched those seen with single gating glutamate mutants (5–7), including a similar anion selectivity and insensitivity to extracellular pH.

Replacing external Cl⁻ with NO₃⁻ or SCN⁻ increased CIC-4 and -5 currents (7, 25, 26). Anion flux through ecCIC-1 is partially or totally uncoupled from H⁺ with transport of NO₃⁻ or SCN⁻, respectively (27). Likewise, CIC-4 and -5 show less H⁺ countertransport with NO₃⁻ or SCN⁻ (Fig. 5, *A* and *B*), with an almost complete loss of H⁺ transport in SCN⁻. However, uncoupling with SCN⁻ has to be viewed with caution, as SCN⁻ also induces rather large currents in uninjected oocytes (supplemental Fig. S4A) and in mock-transfected mammalian cells (data not shown). Quantitatively comparing pH_i changes with the transferred charge confirmed partial uncoupling by NO₃⁻ and SCN⁻ (Fig. 5C). The partial uncoupling of NO₃⁻ or SCN⁻ fluxes from H⁺ transport suggested that these anions might permeate CIC-4 or -5 even when their proton glutamates are replaced with nondissociable residues. However, also with a replacement of extracellular Cl⁻ with NO₃⁻ or SCN⁻, CIC-5_{E268A} failed to give currents differing from uninjected controls (supplemental Fig. S4, *A* and *B*), in contrast to the E268D mutant (supplemental Fig. S4C), which still supports Cl⁻/H⁺ exchange. We did not observe significant currents with the E268A mutant when applying solutions in the pH range from 5.5 to 8.5, even in the presence of NO₃⁻ (data not shown).

We next inserted proton glutamates into CIC-0 and -1. These mutations affected gating, but did not transform those Cl⁻ channels into Cl⁻/H⁺ exchangers, as H⁺ transport was undetectable. Reversal potential measurements confirmed this conclusion (supplemental Fig. S5 and Table 1).

To explore whether the coupled Cl⁻/H⁺ exchange depends on the presence of two fully functional subunits of the CLC, we analyzed concatemers. Currents and pH_o changes of control WT-WT dimers (Fig. 6A) resembled those of WT CIC-5, as did those of concatemers linking a E268A with a WT subunit (Fig. 6B). A concatemer linking a WT subunit to the uncoupled gat-

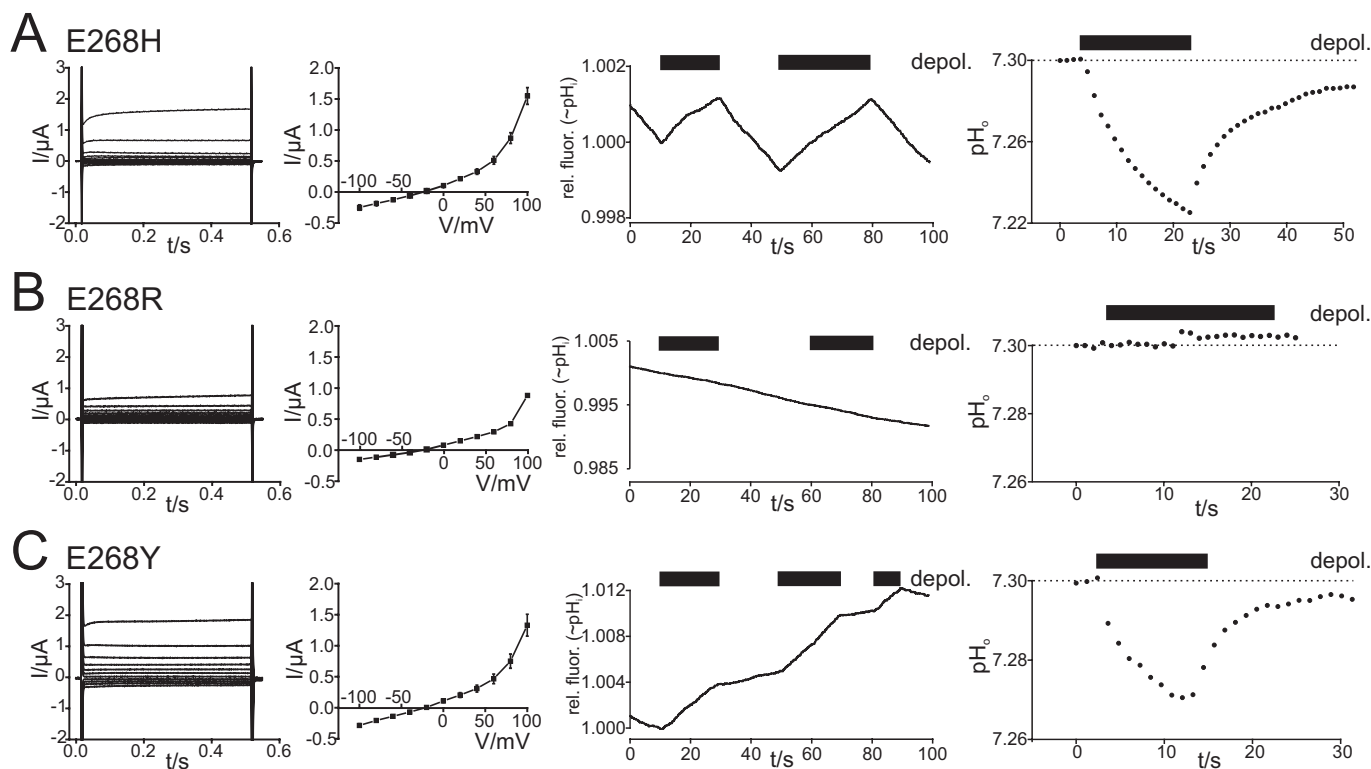


FIGURE 2. Effects of replacing the CIC-5 proton glutamate (Glu-268) with the protonatable residues histidine (A), arginine (B), and tyrosine (C). *Left*, voltage clamp traces of oocytes and corresponding averaged I/V curves ($n = 27$, 14, and 17, respectively). *Middle*, intracellular alkalization detected by Fluorocyte ($n = 24$, 6, and 13, respectively). *Right*, extracellular acidification measured with a pH electrode ($n = 11$, 4, and 4, respectively). *Bars*, trains of depolarizing pulses (depol.) to 90 mV (middle) or 80 mV (right). *rel. fluor.*, relative fluorescence.

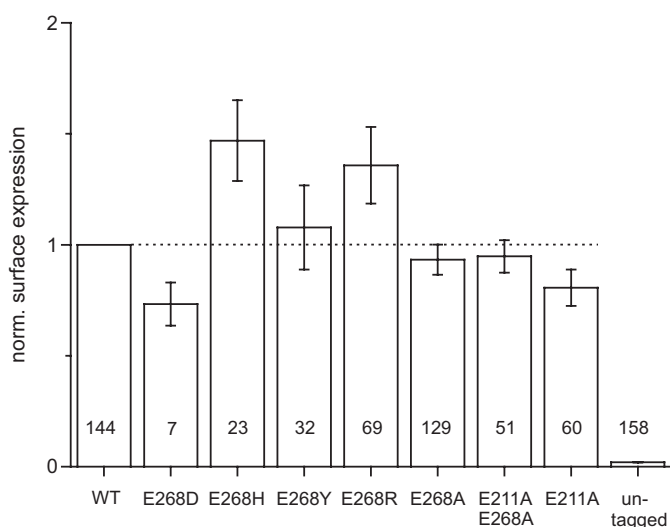


FIGURE 3. Surface expression of WT CIC-5 and mutants in the proton and gating glutamates. Proteins were tagged with extracellular HA epitopes, and surface expression in *Xenopus* oocytes was determined as described under "Experimental Procedures." Data were normalized to those obtained with tagged WT CIC-5 in the same batch of oocytes (left bar). Oocytes expressing untagged WT and E268A mutant CIC-5 were used as a control, with pooled data shown in the right-most bar. The constructs used for expression are shown below the bars, and error bars indicate S.E. Data were from three batches for HA-tagged E268H, E268Y, E268R, E211A, and E211A/E268A; five batches for HA-tagged WT CIC-5 and E268A; one batch for HA-tagged E268D; and five batches for untagged controls.

ing glutamate mutant E211A also transported H^+ (Fig. 6C). It mediated significant currents at negative voltages (Fig. 6, C and D), demonstrating that the E211A subunit is functional and not

qualitatively altered by the WT subunit. These results suggest that a single subunit is able to perform ion exchange independently from the other subunit.

We next performed noise analysis of inside-out patches from CIC-5-expressing oocytes to get more insight in the mechanism of transport. Fig. 7A shows the macroscopic current averages and the corresponding variance. Current relaxations after voltage jumps from 0 to 140 mV could be fitted with a bi-exponential function with time constants of 1.4 ± 0.2 and 13.6 ± 1.6 ms ($n = 6$) (data not shown). Fig. 7B plots the variance against the corresponding mean current. These data were fitted with Equation 1 to estimate the "unitary conductance," even though such an analysis has been developed for ion channels rather than transporters (see "Discussion"). Because current relaxations were small, only a limited range of the parabola (Equation 1) was sampled. Nonetheless, fitting with Equation 1 gave the consistent estimate of 63 ± 8 fA ($n = 6$) for the unitary current at 140 mV, corresponding to a conductance of 0.45 ± 0.06 picosiemens. Fig. 7C shows the spectral analysis of the noise that can be fitted by a three-component lorentzian function with cut-off frequencies of 15.0 ± 4.5 , 217 ± 23 , and 2400 ± 230 Hz, respectively ($n = 6$). Using $\tau = 1/(2\pi f)$, the lower frequencies correspond to time constants of 10.6 and 0.7 ms, respectively, consistent with the time constants of the macroscopic current relaxation. Also the lorentzian appearance of the power spectrum is *a priori* expected for an ion channel but not for a transporter (28).

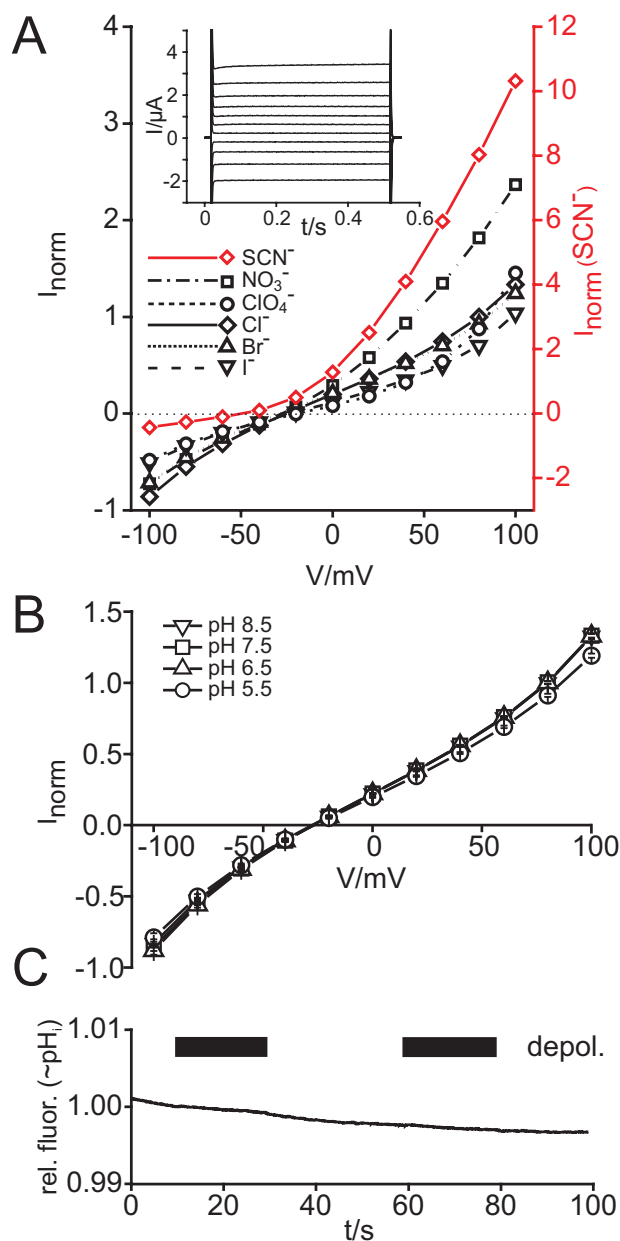


FIGURE 4. Cl^- , but not H^+ , transport is restored in the CIC-5 proton glutamate E268A mutant by the additional uncoupling mutation in the gating glutamate (E211A). *A*, I/V curves of the double mutant with different anions ($n = 20$). *Inset*, voltage clamp traces obtained with Cl^- . SCN^- often induced endogenous currents in *Xenopus* oocytes and transfected cells, in particular at positive voltages (see supplemental Fig. S4A). *B*, changing pH_o affects neither conductance nor reversal potentials, in accord with the lack of H^+ transport observed in Fluorocyte measurements ($n = 21$) (*C*). *depol.*, depolarizing pulse trains; *rel. fluor.*, relative fluorescence.

DISCUSSION

We report several novel findings for CIC-4 and -5. (*a*) Both anion and proton transport depend on an internal proton glutamate, which can be functionally replaced with other dissociable amino acids. (*b*) Transport of polyatomic anions is partially uncoupled from H^+ transport, but still depends on the proton glutamate. (*c*) The insertion of a proton glutamate is not sufficient to convert CLC channels into exchangers. (*d*) Cl^-/H^+ exchange is independent of the associated

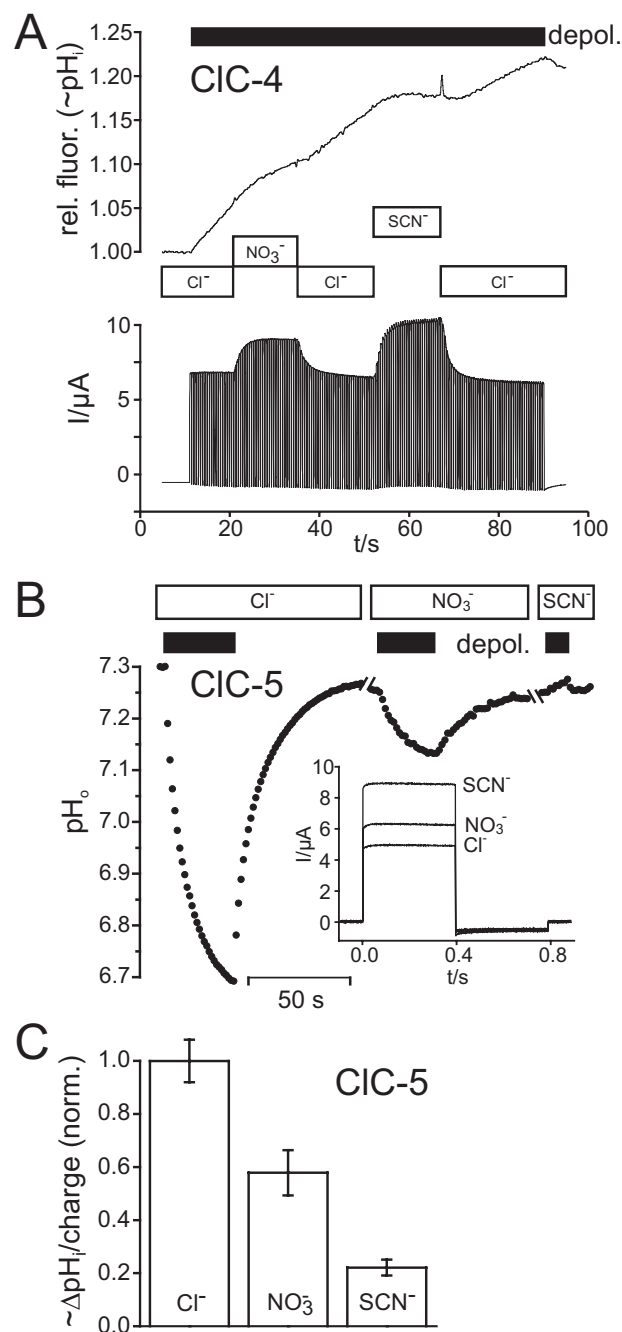


FIGURE 5. Partial uncoupling of Cl^-/H^+ exchange by polyatomic anions. *A*, continuous measurement of pH_i -sensitive fluorescence (*upper trace*) and currents needed to clamp oocytes expressing WT CIC-4 during 400 ms pulses to 90 mV (*lower trace*) during complete exchange of external anions (indicated by bars). Currents are larger with NO_3^- or SCN^- than with Cl^- , but the induced alkalinization rate is smaller. *depol.*, depolarizing pulse trains. *B*, extracellular acidification induced by depolarizing an oocyte expressing WT CIC-5 and typical currents needed to clamp to 80 mV (*inset*). Similar results as in *A* or *B* were obtained with 10 and 14 oocytes each. *C*, ratiometric determination of pH_i during two-electrode voltage clamp with a pulse protocol similar to that described in *A*, but in CIC-5-expressing oocytes. Ratio changes during 10 s of pulses to 90 mV were divided by the transferred charge and normalized to data with Cl^- for a relative measure of exchange stoichiometry ($n = 9, 8,$ and 6 , respectively). *rel. fluor.*, relative fluorescence.

subunit and (*e*) is modulated by a process that resembles gating of channels.

An internal proton glutamate (Glu-203 in ecCIC-1) was proposed (19) to shuttle H^+ from the interior to the gating gluta-

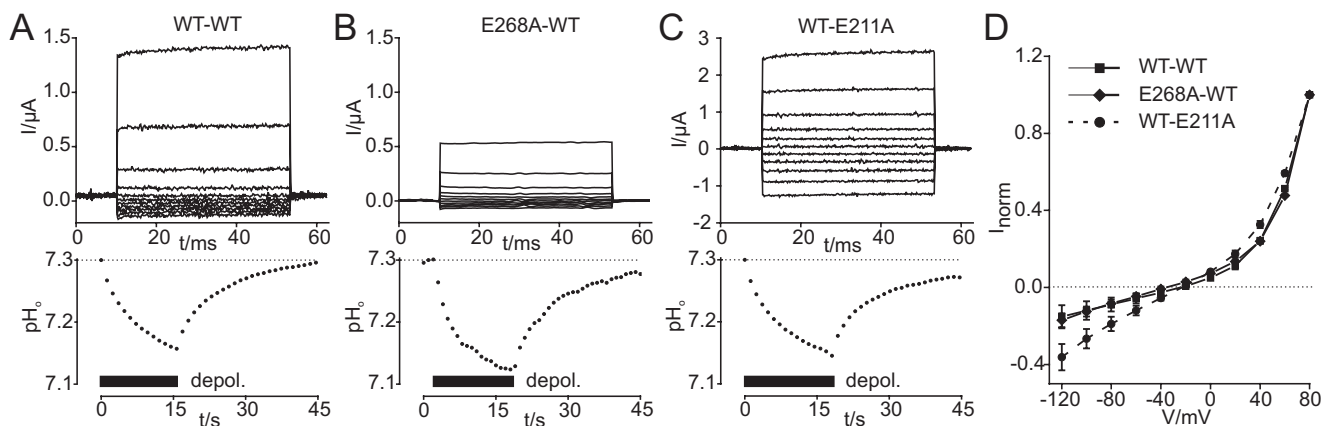


FIGURE 6. **CIC-5 Cl⁻/H⁺ exchange can be mediated independently by each subunit of the dimer.** A–C, typical voltage clamp traces (to 80 mV in 20 mV steps) (upper panels) and external acidification during 80 mV pulse trains (lower panels) for the control WT-WT concatemer (A), the E268A-WT concatemer with a nontransporting proton glutamate mutant (B), and a concatemer with the uncoupled E211A gating glutamate mutant (C) ($n = 13, 7,$ and $6,$ respectively). *depol.*, depolarizing pulse trains. D, current/voltage relationships of WT-WT, E211A-WT, and the E268A-WT concatemers. Currents were normalized to those at 80 mV.

mate (Glu-148), a residue involved in coupling Cl⁻ to H⁺ fluxes and located roughly in the center of CLC monomers. Neutralizing this proton glutamate transformed ecCIC-1 into a pure Cl⁻ conductance. However, if this residue only serves to shuttle protons to and from a Cl⁻/H⁺ exchange site, anion transport should be stalled when the path for H⁺ is obliterated. This was indeed observed here for CIC-4 and -5. An additional uncoupling mutation at the likely exchange site, the gating glutamate, restored anion currents, suggesting that the proton glutamate directly impinges on proton, but not anion, transport. This notion is further strengthened by the (partial) functional replacement of the proton glutamate with other protonatable residues like aspartate, histidine, and tyrosine. With the exception of aspartate, no such replacements were reported for ecCIC-1 (19).

All confirmed CLC Cl⁻/H⁺ exchangers display a proton glutamate, whereas it is replaced with valine in all established CLC Cl⁻ channels. However, insertion of such a glutamate is not sufficient to enable Cl⁻/H⁺ coupling, as evident from our failure to convert CLC channels into exchangers.

Polyatomic anions like SCN⁻, NO₃⁻, and ClO₄⁻ permeate ecCIC-1 with only partial or no coupling to H⁺ (27, 29). We observed similar uncoupling in CIC-4 and -5. If these polyatomic anions can permeate without coupling to H⁺, they also might yield currents when the supply of H⁺ is blocked by proton glutamate mutations. Because this was not observed, mutations in the proton glutamate may affect anion transport not just by preventing anion/H⁺ exchange. Because either glutamate or histidine promoted Cl⁻/H⁺ exchange, electrostatic effects seem unlikely. Probably protonation (or neutralization) of the gating glutamate is essential also for the uncoupled SCN⁻ transport.

CLC proteins function as (homo)dimers with two pores (13, 14, 30). Conduction properties of CLC channels are determined by their monomers (31), but certain gates can close both pores simultaneously. In a similar manner there might be a link between Cl⁻/H⁺ exchange and the dimeric structure. However, our studies of concatemers showed that each subunit can

mediate Cl⁻/H⁺ exchange independently of the transport activity of the second subunit.

We report the first estimate for an apparent unitary conductance of CIC-5. The value of 0.45 ± 0.06 picosiemens is similar to results for CIC-4 (26). Nonstationary noise analysis is usually applied only to ion channels, but has also revealed gating events in the Na⁺/Ca²⁺ exchanger (32). In analogy to the model of Hilgemann (32), we interpret the results of the noise analysis in the following manner. Electrogenic Cl⁻/H⁺ exchange, which occurs at a very high rate, is switched on and off by a gating process. Each burst of transport activity is associated with an electrical conductance of 0.45 picosiemens, as the elementary electrogenic exchange processes cannot be temporally resolved. Such a behavior is qualitatively illustrated in Fig. 8A. The recording bandwidth is not sufficient to resolve individual transport events. The noise at the frequencies that can be measured is thus dominated by the gating of the bursts. Assuming that the unitary current reflects the charge transport rate of a single transporter and assuming a transport stoichiometry of 2Cl⁻/1H⁺ as for ecCIC-1 (4, 27), a transport turnover rate (at 100 mV) of about 10^5 s⁻¹ can be estimated. The turnover rate of ecCIC-1 was estimated to 4000 s⁻¹ at 0 mV (33). If the strong rectification of CIC-5 reflects a voltage dependence of the turnover rate, CIC-5 turnover at less positive voltages may resemble that of ecCIC-1.

As with CLC channels, neutralizing the gating glutamate of CIC-4 or -5 abolished rectification and current relaxations after voltage jumps, possibly suggesting that rectification results from voltage-dependent gating. However, >80% of the current increase upon depolarization is instantaneous. Hence, in a reinterpretation of the results of Hebeisen *et al.* (26), we propose that the major part of rectification stems from an intrinsic voltage dependence of “turned on” Cl⁻/H⁺ exchange. The gating glutamate may need to be protonated to allow anion permeation (15). If protons can reach this glutamate in CIC-4 and -5 only from the intracellular side along a path involving the proton glutamate and must be driven there against an energy barrier by voltage, outward rectification ensues. Fig. 8B schemati-

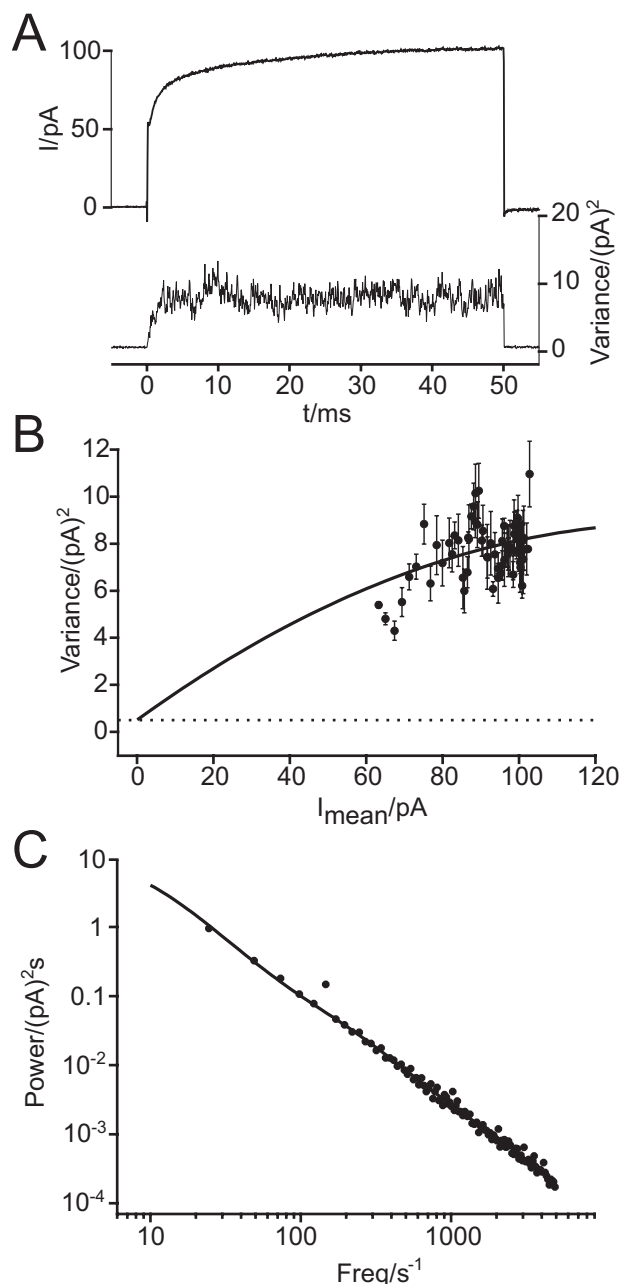


FIGURE 7. **Noise analysis of WT CIC-5.** *A*, average of 100 macroscopic current recordings and corresponding variance from a representative patch. *B*, for the same patch, plot of the variance against the corresponding mean current and fit with Equation 1 (see “Experimental Procedures”). Background variance estimated at -50 mV is shown as a dotted line. *C*, spectral analysis of the noise of data shown in *A* and fit with a three-component lorentzian function as in Equation 2 (see “Experimental Procedures”). Note that the noise spectrum observed is typical for an ion channel and not a transporter.

cally illustrates this scenario. As expected from this model, currents increased exponentially with voltage, in contrast to a gating process, which finally saturates at the maximal open probability of 1. The exponential current increase also implies that neither the supply of H^+ from the cytoplasmic solution to the proton glutamate nor the delivery of H^+ to the extracellular solution is rate-limiting.

In contrast to CIC-4 and -5, currents of ecCIC-1 are linear, and mutations in its proton glutamate abolish H^+ coupling

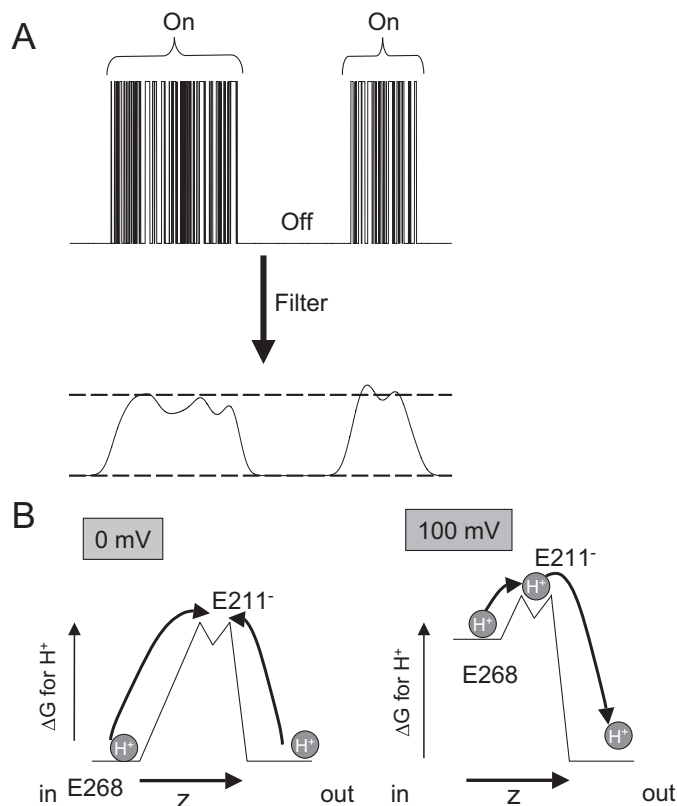


FIGURE 8. **Models of transport mechanisms in CIC-4 and CIC-5.** *A*, hypothetical currents generated by bursts of transport activity at infinite time resolution (*top trace*) and after filtering (*bottom trace*) are shown to illustrate our interpretation of the noise analysis. The spectral properties of CIC-5 are consistent with a (speculative) model that assumes that transport activity occurs in bursts (indicated by *on*) during which transport occurs at a rate that is not spectrally resolved. Filtering results in an averaged transporter current that is qualitatively correlated with the maximal turnover rate. The shape of the experimentally determined power spectrum is dominated by the gating of the burst. *B*, the strong rectification of CIC-4- and CIC-5-mediated currents could be explained by a model in which transport is rate-limited by proton transfer to Glu-211, which is kinetically disfavored due to a high energy barrier. The barrier can be overcome at large positive voltages that favor proton delivery from Glu-268. If the gating glutamate is electrically closer to the external solution, as shown in the figure, outward rectification ensues.

without eliminating anion currents. The interpretation of these data is complicated by the nonuniform orientation of the reconstituted transporter in the lipid bilayer. However, if protons could reach the gating glutamate of ecCIC-1 also from the exterior, both the lack of rectification and the uncoupled anion currents with proton glutamate mutations would be explained.

Acknowledgments—We thank A. Fast, L. Ferrera, and M. Petersen for technical assistance; G. Gaggero and S. Wendt for help in construction of the perfusion chambers; and E. Gaggero and G. Gaggero for building the high-impedance amplifier.

REFERENCES

- Jentsch, T. J., Stein, V., Weinreich, F., and Zdebik, A. A. (2002) *Physiol. Rev.* **82**, 503–568
- Zifarelli, G., and Pusch, M. (2007) *Rev. Physiol. Biochem. Pharmacol.* **158**, 23–76
- Jentsch, T. J., Steinmeyer, K., and Schwarz, G. (1990) *Nature* **348**, 510–514
- Accardi, A., and Miller, C. (2004) *Nature* **427**, 803–807

5. Picollo, A., and Pusch, M. (2005) *Nature* **436**, 420–423
6. Scheel, O., Zdebik, A., Lourdel, S., and Jentsch, T. J. (2005) *Nature* **436**, 424–427
7. Friedrich, T., Breiderhoff, T., and Jentsch, T. J. (1999) *J. Biol. Chem.* **274**, 896–902
8. Jentsch, T. J. (2007) *J. Physiol. (Lond.)* **578**, 633–640
9. Lloyd, S. E., Pearce, S. H., Fisher, S. E., Steinmeyer, K., Schwappach, B., Scheinman, S. J., Harding, B., Bolino, A., Devoto, M., Goodyer, P., Rigden, S. P., Wrong, O., Jentsch, T. J., Craig, I. W., and Thakker, R. V. (1996) *Nature* **379**, 445–449
10. Miller, C., and White, M. M. (1984) *Proc. Natl. Acad. Sci. U. S. A.* **81**, 2772–2775
11. Bauer, C. K., Steinmeyer, K., Schwarz, J. R., and Jentsch, T. J. (1991) *Proc. Natl. Acad. Sci. U. S. A.* **88**, 11052–11056
12. Lorenz, C., Pusch, M., and Jentsch, T. J. (1996) *Proc. Natl. Acad. Sci. U. S. A.* **93**, 13362–13366
13. Ludewig, U., Pusch, M., and Jentsch, T. J. (1996) *Nature* **383**, 340–343
14. Dutzler, R., Campbell, E. B., Cadene, M., Chait, B. T., and MacKinnon, R. (2002) *Nature* **415**, 287–294
15. Dutzler, R., Campbell, E. B., and MacKinnon, R. (2003) *Science* **300**, 108–112
16. Waldegger, S., and Jentsch, T. J. (2000) *J. Biol. Chem.* **275**, 24527–24533
17. Niemeyer, M. I., Cid, L. P., Zuñiga, L., Catalán, M., and Sepúlveda, F. V. (2003) *J. Physiol. (Lond.)* **553**, 873–879
18. Pusch, M., Ludewig, U., Rehfeldt, A., and Jentsch, T. J. (1995) *Nature* **373**, 527–531
19. Accardi, A., Walden, M., Nguiragool, W., Jayaram, H., Williams, C., and Miller, C. (2005) *J. Gen. Physiol.* **126**, 563–570
20. Steinmeyer, K., Schwappach, B., Bens, M., Vandewalle, A., and Jentsch, T. J. (1995) *J. Biol. Chem.* **270**, 31172–31177
21. Koch, M. C., Steinmeyer, K., Lorenz, C., Ricker, K., Wolf, F., Otto, M., Zoll, B., Lehmann-Horn, F., Grzeschik, K. H., and Jentsch, T. J. (1992) *Science* **257**, 797–800
22. Schwake, M., Friedrich, T., and Jentsch, T. J. (2001) *J. Biol. Chem.* **276**, 12049–12054
23. Zerangue, N., Schwappach, B., Jan, Y. N., and Jan, L. Y. (1999) *Neuron* **22**, 537–548
24. De Angeli, A., Monachello, D., Ephritikhine, G., Frachisse, J. M., Thomine, S., Gambale, F., and Barbier-Brygoo, H. (2006) *Nature* **442**, 939–942
25. Vanoye, C. G., and George, A. G., Jr. (2002) *J. Physiol. (Lond.)* **539**, 373–383
26. Hebeisen, S., Heidtmann, H., Cosmelli, D., González, C., Poser, B., Latorre, R., Alvarez, O., and Fahlke, C. (2003) *Biophys. J.* **84**, 2306–2318
27. Nguiragool, W., and Miller, C. (2006) *J. Mol. Biol.* **362**, 682–690
28. Kolb, H. A., and Frehland, E. (1980) *Biophys. Chem.* **12**, 21–34
29. Accardi, A., Lobet, S., Williams, C., Miller, C., and Dutzler, R. (2006) *J. Mol. Biol.* **362**, 691–699
30. Middleton, R. E., Pheasant, D. J., and Miller, C. (1996) *Nature* **383**, 337–340
31. Weinreich, F., and Jentsch, T. J. (2001) *J. Biol. Chem.* **276**, 2347–2353
32. Hilgemann, D. W. (1996) *Biophys. J.* **71**, 759–768
33. Walden, M., Accardi, A., Wu, F., Xu, C., Williams, C., and Miller, C. (2007) *J. Gen. Physiol.* **129**, 317–329